ELSEVIER

Journal of Molecular Catalysis A: Chemical 181 (2002) 137–142

JOURNAL OF MOLECULAR CATALYSIS A: CHEMICAL

www.elsevier.com/locate/molcata

Highly active and stable Ni/Ce–ZrO_2 catalyst for H_2 production from methane

Hyun-Seog Roh [a,b], Ki-Won Jun [a], Wen-Sheng Dong [a], Jong-San Chang [a], Sang-Eon Park [a,*], Yung-Il Joe [b]

[a] *Catalysis Center for Molecular Engineering, Korea Research Institute of Chemical Technology, P.O. Box 107, Yusong, Taejon 305-600, South Korea*

[b] *Department of Chemical Engineering, Yonsei University, Seoul 120-749, South Korea*

Received 23 January 2001; received in revised form 9 April 2001; accepted 22 June 2001

Abstract

Steam reforming of methane has been carried out aimed at the development of new and highly active catalysts for H_2 production. The catalytic properties of Ni catalysts supported on various supports have been investigated in connection with characterization results obtained from XRD, H_2 chemisorption, TPR and CO_2-TPD. Among the catalysts examined, Ni/Ce–ZrO_2 exhibited the best activity and stability. The remarkable catalytic performance is interpreted as a combined result of high oxygen storage capacity of ceria in Ce–ZrO_2, strong interaction between Ni and Ce–ZrO_2, basic property of the catalyst and rather high capability of H_2 uptake.

Keywords: CO_2-TPD; Hydrogen chemisorption; Hydrogen production; Ni/Ce–ZrO_2; Steam reforming of methane; TPR

1. Introduction

Hydrogen production has received much attention in recent years because hydrogen is considered as a clean energy source and its demand has increased in chemical industry [1–3]. Steam reforming of methane (SRM) is a widely practiced technology for hydrogen production [4,5]. Conventionally, steam reforming catalysts use supports such as alumina and magnesium-aluminate due to their stabilities at high temperature [5]. However, a large amount of energy is necessary because SRM is highly endothermic reaction and excess steam is introduced to prevent carbon formation. As a consequence of excess steam, the cost of operating SRM plant increases, H_2/CO ratio (>3) increases and CO yield decreases. Therefore, from the industrial point of view, it is necessary to develop new catalysts exceeding commercial steam reforming catalysts in activity and stability so that they can be employed under severe conditions such as high gas hourly space velocity (GHSV). Moreover, catalytic engineering is required to reduce the size and weight of the reactor for on-site H_2 production, especially for the fuel cell application. To make the small equipment, a highly active catalyst is necessary so that it can give almost complete conversion even at very high space velocity and it should be stable enough to endure at high temperature.

Very recently, we have successfully applied zirconia support to CO_2 reforming of methane [6,7]. Moreover, we have also successfully applied Ni/Ce–ZrO_2 to partial oxidation of methane (POM) reaction [8]

* Corresponding author. Tel.: +82-42-860-7670; fax: +82-42-860-7676.
E-mail address: separk@pado.krict.re.kr (S.-E. Park).

1381-1169/02/$ – see front matter
PII: S1381-1169(01)00358-2

and oxy-SRM reaction [9]. Based on the previous results, in this study, we have applied Ni/Ce–ZrO_2 to the steam reforming reaction at high GHSV condition aiming at the development of a suitable catalyst for a compact system of on-site H_2 generation.

2. Experimental

2.1. Catalyst preparation

Supports employed in this study were α-Al_2O_3 (99.5%, Strem Chemicals), SiO_2 (99%, PQ Corp.), $MgAl_2O_4$ (99%, Johnson Matthey), CeO_2 (99%, Aldrich Chemicals), monoclinic ZrO_2 (99%, Strem Chemicals), and Ce-doped ZrO_2. Ce-doped zirconia support (CeO_2/ZrO_2 wt. ratio, 1:4) was prepared by sol–gel method using the mixture of zirconyl chloride and the corresponding salt of Ce [7–9]. The modified zirconia support was calcined at 800 °C for 6 h in air. Ni (15 wt.%) catalysts were prepared by molten-salt method using its nitrate source [10]. The catalyst samples were calcined at 550 °C for 6 h in air.

2.2. Catalyst characterization

The BET specific surface areas were measured by nitrogen adsorption at 77 K (Micromeritics, ASAP-2400). XRD patterns were recorded using a Rigaku 2155D6 diffractometer (Ni-filtered Cu Kα, 40 kV, 50 mA).

H_2 uptake was measured using pulse technique. About 200 mg of catalyst was placed in a quartz reactor. Prior to pulse chemisorption, the sample was reduced in 5% H_2/Ar at 700 °C for 3 h. Then the sample was purged in Ar at 720 °C for 1 h and cooled to 50 °C in flowing Ar. A hydrogen pulse (5% H_2/Ar, 1 ml) was injected into the catalysts at 50 °C. The calculation methods of metal dispersion, surface area and average crystallite diameter are same as that in reference [11] by assuming the adsorption stoichiometry of one hydrogen atom per nickel surface atom ($H/Ni_s = 1$).

Temperature programmed reduction (TPR) experiments were carried out in a conventional apparatus. Typically, 50 mg of precalcined sample was loaded into quartz reactor. The TPR was performed using 5% hydrogen in nitrogen, 15 ml/min, with a heating rate of 10 °C/min, from 100 to 900 °C. The sensitivity of the detector was calibrated by reducing known weight of NiO. H_2 consumption was obtained from the integrated peak area of the reduction profiles relative to the calibration curve.

CO_2 temperature programmed desorption (TPD) experiment was carried out using a flow system equipped with a thermal conductivity detector (TCD). Prior to the experiment, the sample was pretreated at 700 °C for 1 h in He. Then it was cooled down and CO_2 was adsorbed at 50 °C. After being purged with He to remove the weakly adsorbed CO_2, the sample was heated again from 50 to 650 °C at a heating rate of 10 °C/min in He flow.

2.3. Catalytic reaction

Catalytic activity measurements were conducted in a fixed-bed quartz reactor with inner diameter of 4 mm at atmospheric pressure. About 50 mg of each catalyst was loaded into a quartz reactor. The reaction temperature was measured and controlled by a thermocouple inserted directly into the top layer of the catalyst bed. Prior to each catalytic measurement, the catalyst was reduced in H_2/N_2 (5% H_2 in vol.) at 700 °C for 2 h. The reactant gas stream consisted of CH_4 and H_2O with a molar ratio of 1:3. H_2O was injected using a micro-syringe pump, and evaporated at 300 °C in a preheating zone. N_2 was introduced with the flow rate of 30 cm^3/min as a reference gas for GC analysis. Effluent gases from the reactor were analyzed by a gas chromatograph (Chrompack CP9001) equipped with a TCD and a CarboPLOT P7 column.

In this study, H_2 yield and CO yield were defined considering only the steam reforming reaction as shown in the following equations.

$$H_2\ \text{yield}\ (\%) = (\text{moles of } H_2 \text{ formed}/\text{moles of } CH_4 \text{ fed} \times 3) \times 100 \quad (1)$$

$$\text{CO yield}\ (\%) = (\text{moles of CO formed}/\text{moles of } CH_4 \text{ fed}) \times 100 \quad (2)$$

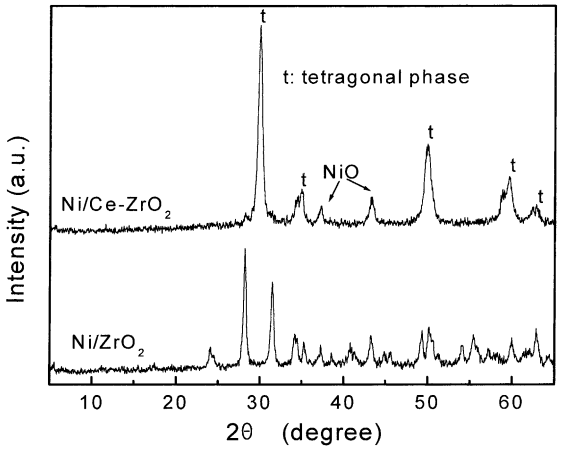

Fig. 1. XRD patterns of Ni/Ce–ZrO_2 and Ni/ZrO_2 catalysts.

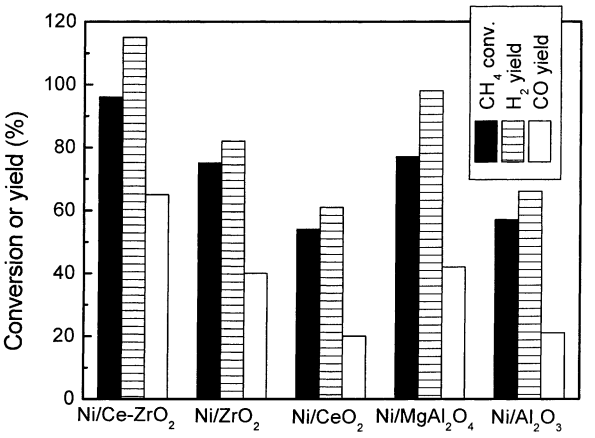

Fig. 2. Activity comparison for supported Ni catalysts (reaction conditions: $P = 1$ atm, $T = 750°C$, $H_2O/CH_4 = 3.0$, GHSV $= 144{,}000\ cm^3/g_{cat}\ h$).

3. Results and discussion

3.1. Characteristics of the catalysts

Fig. 1 illustrates the XRD patterns of Ni/Ce–ZrO_2 and Ni/ZrO_2. Whereas Ce–ZrO_2 solid solution in Ni/Ce–ZrO_2 is identified as a tetragonal phase, the XRD pattern of Ni/ZrO_2 shows characteristic peaks of monoclinic phase.

Table 1 summarizes BET surface area, H_2 uptake, metallic Ni dispersion, surface area and average crystallite diameter of Ni. The dispersion data indicate that Ni particles are better dispersed on $MgAl_2O_4$, ZrO_2, and Ce–ZrO_2 than on Ni/Al_2O_3 and Ni/CeO_2. The latter do not adsorb hydrogen.

3.2. Catalytic performance

Various Ni catalysts (Ni content: 15 wt.%) on supports mentioned above were examined at 750 °C and space velocity of $144{,}000\ cm^3/g_{cat}\ h$ for CH_4 conversion, H_2 yield, and CO yield (Fig. 2). Ni/SiO_2 showed a low initial activity (23% CH_4 conversion). Its activity decreased dramatically with time on stream, and after 60 min it showed no activity. This indicates that Ni/SiO_2 system does not have high activity in SRM or hydrothermal stability either. It is likely that there is an interaction between silica and Ni resulting in the deactivation of the catalysts. Ni/Al_2O_3 catalyst showed rather high activity (72% CH_4 conversion) at the initial stage, but the activity decreased gradually with increasing time. It showed 57% CH_4 conversion after 200 min. It would be due to the fact that SRM reaction in this work was operated with rather lower H_2O/C ratio than that in commercial processes. On the Ni/Al_2O_3 catalyst, carbon was deposited slowly, and thus the catalyst was deactivated gradually. In contrast to these two systems, Ni/$MgAl_2O_4$ showed high activity (79% CH_4 conversion) as well as high stability. Because $MgAl_2O_4$ is less acidic than Al_2O_3, less coke is formed on it resulting in high stability.

Table 1
Characteristics of supported Ni catalysts

Catalyst	Surface area (m^2/g)	H_2 uptake ($\mu mol/g_{cat}$)	Dispersion (%)	Surface area of Ni (m^2/g)	Average crystallite diameter (nm)
Ni/Ce–ZrO_2	40	9.39	0.86	0.76	112
Ni/ZrO_2	13	12.78	1.07	1.04	90.1
Ni/CeO_2	3	0.0	–	–	–
Ni/$MgAl_2O_4$	18	24.1	2.23	1.96	43
Ni/Al_2O_3	1	0.0	–	–	–

Ni/CeO_2 did not show high activity, but the activity was maintained as time on stream increased. Ni/ZrO_2 showed high activity (77% CH_4 conversion) and high thermal stability also. $Ni/Ce–ZrO_2$ showed the highest activity (97% CH_4 conversion) as well as high stability. The H_2 concentration in the reactor effluent was 62%. The values of CH_4 conversion and H_2 concentration reached very close to their own equilibrium values (CH_4 conversion: 99.4% and H_2 concentration: 62.7%).

$Ni/Ce–ZrO_2$ showed the highest H_2 yield among the tested catalysts. It showed the 115% yield, which indicates that the quantity of hydrogen obtained exceeds the limit which is obtainable only from SRM. It is due to the water gas shift (WGS) reaction resulting from excess supply of steam. This also explains the fact that H_2 yield is always higher than CH_4 conversion irrespective of catalyst. However, all the other catalysts gave hydrogen yield below 100%.

CO yields were relatively low (<70%) because of the WGS reaction. The values were relatively high at the initial stage of the reaction time, and they decreased gradually. The values reached a steady state after 100 min.

H_2/CO and $H_2/(CO + CO_2)$ ratios are summarized in Table 2. The trends of H_2/CO ratio were opposite to those of methane conversion or hydrogen yield. The lower H_2/CO ratio was observed, as the higher CH_4 conversion was attained. On the catalysts, $Ni/Ce–ZrO_2$, Ni/ZrO_2 and $Ni/MgAl_2O_4$, about 3.5 mol of hydrogen was produced per 1 mol of methane reacted in SRM. The higher value than 3 indicates that WGS reaction was carried out as a side reaction during SRM reaction. In the case of Ni/CeO_2, the highest H_2/CO ratio was observed, implying that considerable WGS reaction was executed.

Table 2
H_2/CO ratio and $H_2/(CO + CO_2)$ over supported Ni catalysts in SRM[a]

Catalyst	H_2/CO		$H_2/(CO + CO_2)$	
	144,000[b]	288,000	144,000	288,000
$Ni/Ce–ZrO_2$	4.9	7.1	3.4	3.7
Ni/ZrO_2	6.3	7.8	3.4	3.8
Ni/CeO_2	11.1	38.0	3.8	3.9
$Ni/MgAl_2O_4$	6.4	9.2	3.5	3.8
Ni/Al_2O_3	10.1		3.7	

[a] Reaction data obtained at time on stream: 200 min.
[b] GHSV (cm^3/g_{cat} h).

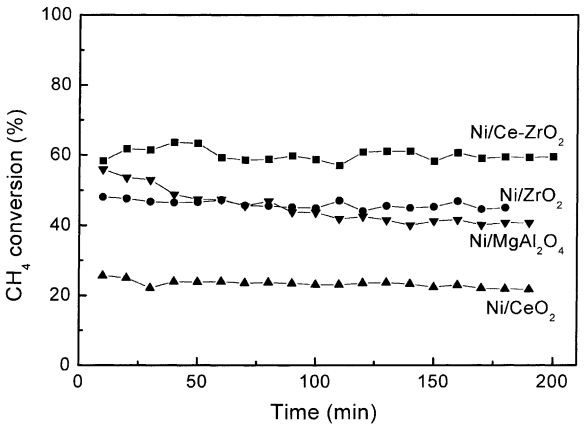

Fig. 3. Activity changes of supported Ni catalysts depending on time on stream at high GHSV (reaction conditions: $P = 1$ atm, $T = 750°C$, $H_2O/CH_4 = 3.0$, GHSV = 288,000 cm^3/g_{cat} h).

In order to investigate the activity and the stability at high GHSV, CH_4 conversions with time on stream were recorded at 288,000 cm^3/g_{cat} h over $Ni/Ce–ZrO_2$, Ni/ZrO_2, Ni/CeO_2, and $Ni/MgAl_2O_4$ (Fig. 3). All the catalysts tested at this condition showed stable activity at 144,000 cm^3/g_{cat} h. However, in this high GHSV, $Ni/MgAl_2O_4$ did not show stability. Its CH_4 conversion was initially 56%, but it decreased to 40% after 3 h. This catalyst does not have stability at high GHSV (>288,000 cm^3/g_{cat} h). In contrast to this catalyst, the others showed stable activities regardless of the initial activities. H_2/CO and $H_2/(CO + CO_2)$ ratios under this condition are also summarized in Table 2. H_2/CO ratios at 288,000 cm^3/g_{cat} h were higher than those at 144,000 cm^3/g_{cat} h. The WGS reaction became predominant at this high GHSV resulting in low CO yield, because relatively a large amount of unreacted steam reacts with relatively a small amount of CO produced.

According to the above results, $Ni/Ce–ZrO_2$ showed the highest activity and excellent stability, showing the possibility that it can replace the widely employed $Ni/MgAl_2O_4$ steam reforming catalysts.

3.3. TPR results

TPR patterns on pure NiO and supported Ni catalysts are presented in Fig. 4. The calculated total

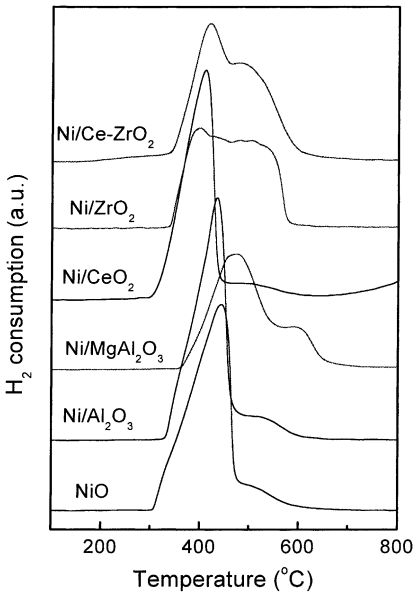

Fig. 4. TPR patterns of supported Ni catalysts.

hydrogen consumption (THC), support hydrogen consumption (SHC) and reduction degree of Ni from TPR results are also summarized in Table 3. Generally, for supported Ni catalysts the lower temperature peaks are attributed to the reduction of the relatively free NiO particles, while the higher temperature peaks are assigned to the reduction of complex NiO species in intimate contact with the oxide support. Pure NiO shows sharp reduction peak at about 420 °C followed by a small hump. The TPR curve of Ni/Al_2O_3 is similar to that of pure NiO, indicating that there is no strong interaction between NiO and Al_2O_3 support. In the case of $Ni/MgAl_2O_4$, the maximum peak shifts toward the high temperature (470 °C) followed by a small peak at 620 °C. This suggests that there are two kinds of NiO species. The first peak can be assigned to relatively free NiO weakly interacting with support, and the second peak is attributable to complex NiO strongly interacting with support. Ni/CeO_2 shows sharp reduction peak at about 420 °C followed by a small tail. At 880 °C, a broad peak appears attributed to partial reduction of CeO_2, which is consistent with the TPR curve of only CeO_2 support [8,9]. Thus, there is no strong interaction between NiO and CeO_2. For Ni/ZrO_2, broad and unresolved reduction peaks with maxima at about 400 and 510 °C are observed.

$Ni/Ce–ZrO_2$ exhibits two peaks without any obvious peak at 640 °C. This is possibly due to the fact that strong interaction between Ni and $Ce–ZrO_2$ makes ceria more reducible, which probably helps to produce mobile oxygen during the reforming reaction. The first sharp peak can be assigned to relatively free NiO and the second broad peak to complex NiO species which strongly interact with $CeZrO_2$, and it seems to be concurrent with ceria reduction. The reducibility of the support is most likely to be related with the abundance of mobile oxygen. $Ce–ZrO_2$ solid solution has a higher concentration of mobile oxygen than CeO_2 or ZrO_2 [9].

Table 3
TPR results on supported Ni catalysts

Catalysts	THC[a] ($mmol/g_{cat}$)	SHC[b] ($mmol/g_{cat}$)	Reduction degree of Ni (%)
$Ni/Ce–ZrO_2$	5.03	0.70	84.7
Ni/ZrO_2	4.73	0	92.5
Ni/CeO_2	4.49	0	87.8
$Ni/MgAl_2O_4$	4.29	0	83.9
Ni/Al_2O_3	4.94	0	96.7

[a] Total hydrogen consumption in TPR over supported Ni catalysts.
[b] Hydrogen consumption of support in Ni/supports.

3.4. CO_2 TPD results

CO_2 TPD results on the supported Ni catalysts are illustrated in Fig. 5. Ni/Al_2O_3 shows a desorption peak at 100 °C. $Ni/MgAl_2O_4$ presents large desorption peak at 150 °C. Ni/CeO_2 has a desorption peak at 100 °C, which is same as that of Ni/Al_2O_3 but the peak intensity is large and it has a long tail, indicating continuous desorption or dissociation of CO_2 up to 500 °C. In the case of Ni/ZrO_2, a strong peak at 130 °C appears followed by a big tail and a small peak at 500 °C. $Ni/Ce–ZrO_2$ exhibits three peaks at 130, 350, and 490 °C, respectively. The areas under the peaks at 350 and 490 °C increase with the addition of Ce, suggesting that both the medium and strong basic sites increase with the addition of Ce to ZrO_2.

The high oxygen storage capacity of ceria in $Ce–ZrO_2$ solid solution enables it to store and release reversibly a large amount of active oxygen species. In addition, basic sites strongly inhibit carbon formation. Finally, the high adsorption of H_2 promotes the methane reforming reactions.

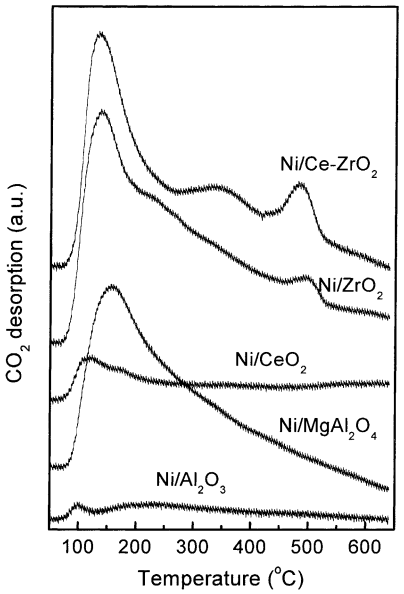

Fig. 5. CO_2-TPD patterns of supported Ni catalysts.

4. Conclusions

Based on the above results, the following conclusions are drawn.

1. Ni/Ce–ZrO_2 showed outstanding activity and stability.
2. The remarkable catalytic performance of Ni/Ce–ZrO_2 is attributed to the combination of several advantages, i.e. high oxygen storage capacity of ceria in Ce–ZrO_2 solid solution, strong interaction between Ni and Ce–ZrO_2, basic property, and rather high capability for H_2 uptake.

References

[1] M.A. Peña, J.P. Gómez, J.L.G. Fierro, Appl. Catal. A 144 (1996) 7.
[2] J.N. Armor, Appl. Catal. A 176 (1999) 159.
[3] S.C. Tsang, J.B. Claridge, M.L.H. Green, Catal. Today 23 (1995) 3.
[4] J.R. Rostrup-Nielsen, in: J.R. Anderson, M. Boudart (Eds.), Catalysis, Science and Technology, Vol. 5, Springer, Berlin, 1984, p. 1.
[5] D.E. Ridler, M.V. Twigg, in: M.V. Twigg (Ed.), Catalyst Handbook, 2nd Edition, Wolfe Publishing Ltd., England, 1989, p. 225 (Chapter 5).
[6] X. Li, J.-S. Chang, S.-E. Park, Chem. Lett. (1999) 1099.
[7] X. Li, J.-S. Chang, M. Tian, S.-E. Park, Appl. Organometal. Chem. 15 (2001) 109.
[8] H.-S. Roh, W.-S. Dong, K.-W. Jun, S.-E. Park, Chem. Lett. (2001) 88.
[9] H.-S. Roh, K.-W. Jun, W.-S. Dong, S.-E. Park, Y.-S. Baek, Catal. Lett. (2001), in press.
[10] J.-S. Chang, S.-E. Park, H. Chon, Appl. Catal. A 145 (1996) 111.
[11] C.H. Bartholomew, R.B. Pannell, J. Catal. 65 (1980) 390.